The Journal of Supercritical Fluids 174 (2021) 105267

Contents lists available at ScienceDirect

The Journal of Supercritical Fluids

journal homepage: www.elsevier.com/locate/supflu

Efficiency and energetic analysis of the production of gaseous green fuels from the compressed steam and supercritical water gasification of waste lube oils

Ana M. Sanchez-Hernandez, Nicolas Martin-Sanchez, M. Jesus Sanchez-Montero*, Carmen Izquierdo, Francisco Salvador

Dpto. Química Física, Facultad de Ciencias Químicas, Universidad de Salamanca, Plaza de la Merced, s/n 37008 Salamanca, Spain

HIGHLIGHTS

- H_2 and CH_4 are obtained from steam reforming and supercritical water gasification of waste lube oils.
- More than 70% of the energy contained in the waste lube oil can be recovered as H_2 and CH_4.
- The valorization is energetically more efficient when H_2 and CH_4 are the main products obtained.
- H_2 and CH_4 production are promoted at high temperatures and long reaction times.
- Diverse influence of pressure on kinetics, H_2 and CH_4 production, and energy efficiency are analyzed.

GRAPHICAL ABSTRACT

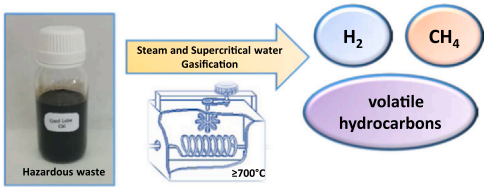

ARTICLE INFO

Keywords:
Hydrogen
Methane
Volatile hydrocarbons
Automotive engine oil

ABSTRACT

The gasification of a waste lube oil (WLO), using water under vapor and supercritical states leads to its valorization into green fuels with high energetic power like H_2 and CH_4. This work investigates how the most important variables of a flow continuous gasification process, temperature, pressure and reaction time, influence the efficiency of gasification and the amounts and characteristics of the gases produced. The study of the influence of these variables on the energetic efficiency of the process was also completed. The highest production yields, 2.4 10^{-2} mol_{H2} g_{oil}^{-1} and 3.0 10^{-2} mol_{CH4} g_{oil}^{-1}, were registered at supercritical water conditions (750 °C, 250 bar and 1.87 min). The energetic study revealed that the energetic efficiency increased as the reaction time was lengthened. Gasification kinetics were slower as pressure increased but the reaction times inside the flow reactor were longer. A pressure range from 150 bar, steam region, to 250 bar, supercritical region, was identified as optimal since allowed the most suitable balance between kinetics and the reaction times achieved.

* Corresponding author.
E-mail addresses: anamsh@usal.es (AM. Sanchez-Hernandez), nicolas_martin@usal.es (N Martin-Sanchez), chusan@usal.es (MJ. Sanchez-Montero), misiego@usal.es (C Izquierdo), salvador@usal.es (F Salvador).

https://doi.org/10.1016/j.supflu.2021.105267
Received 17 December 2020; Received in revised form 6 April 2021; Accepted 16 April 2021
Available online 26 April 2021

1. Introduction

Automotive engine oils are consumed for the internal protection of engines. Usually, 90% of their composition is made of petroleum fractions while the remaining 10% are additives like antioxidants and anti-wear agents [1]. They must be regularly replaced since the severe temperature and friction they are subjected to degrade and pollute the oil with heavy metals, soot and aromatic hydrocarbons [2]. The inappropriate use and removal of the generated waste lube oils (WLOs) can cause huge damages to the environment and human health. The decision 2014/955/EU of the European Commission indicates clearly that WLOs should be classified as hazardous waste since the substances that they contain are classified within categories HP5 (specific organ toxicity), HP 7 (carcinogenic) and HP4 (ecotoxic) [3].

For several years, the energy contained in WLOs has been recovered by combustion and incineration. These techniques remove the residue but are not considered as the best option for the environment due to the emission of different toxic and greenhouse gases [2,4]. The investigations are currently exploring other alternatives like regeneration and valorization. Oladimeji et al. discuss about some of the current regeneration methods of WLOs that allow the reuse of the lubricant, like vacuum distillation, hydrofinishing process or solvent extraction [5]. The valorization alternative makes the most of the energetic power of the WLOs generating valuable fuels. In this field, the technology of pyrolysis and its variants are the most investigated [6–10]. These processes are usually focused on turning the WLOs into secondary fuels similar to diesel. Their use as second-generation fuels reduce the consumption of primary fuels [2], although the products obtained by pyrolysis also contribute to global warming and greenhouse effect because of the types of gases generated in their combustion. Obtaining clean fuels like CH_4 and above all, H_2, is then becoming necessary to face this problem since the atmospheric emissions produced in their combustion are less harmful that those produced by other fuels.

Hydrogen can be produced through different methods like water electrolysis, solar light photoelectrolysis, natural gas steam reforming, coal or biomass gasification [11–15]. Steam catalytic reforming of natural gas/methane is one of the most wide-spread methods [13,16,17]. Large reactors must be employed due to the slow kinetics of the process and when catalysts are used to accelerate it, they are easily deactivated [18]. Methane is the main component of natural gas, one of the most globally demanded fuels. It provides a relative clean combustion thanks to its low ratio C/H [19–21]. Methane is also obtained through different technologies like power to gas (electrolysis of water plus methanation) [22], a combination of coal or biomass gasification and methanation [23,24] anaerobic digestion of biomass [25] or microbial methanogenesis of coal [26].

In spite of the existence of several methods that produce H_2 and CH_4, the search for new environmentally friendly alternatives that support a sustainable energetic development keeps being necessary. Regarding this situation, the current work studies an attractive approach, the valorization of WLOs into green fuels through their gasification with compressed water steam and supercritical water (SCW). These processes can offer important advantages regarding the production of H_2. This species is produced in greater amounts when reforming reactions take place so the use of water, either in steam or supercritical state, seems an interesting option. Specifically, it has been stated that when some typical reforming reactions such as the water-gas shift reaction are carried out under supercritical conditions [27], their kinetics are faster and the achieved conversions are greater thanks to the especial nature and properties of SCW. Namely, the changes that the properties of water experience beyond the critical point (P_c = 221 bar and T_c = 374 °C) turn SCW into a favorable medium for the valorization of organic waste. Complex organic compounds, hydrocarbons and gases are dissolved in SCW, what results in homogeneous reaction and low mass-transfer resistance [28]. The gas-like viscosity of water at supercritical conditions increases its diffusion coefficient and reaction rates. Furthermore, supercritical pressures enhance particle collision and the possibility of chemical reaction to occur within the reactants [29]. Then, despite the difficultness and the high investment of the scale-up of this technology, it may result in high H_2 production yields in comparison with other gasification alternatives. This technology is also considered as environmentally friendly since it does not use organic solvents, catalysts, or any other reagents apart from water. This friendly character is even more marked in this case since the green fuels are produced from the abundant and toxic residue WLO as raw material.

This valorization method has received scarce attention in spite of its potential. As far as we know, only Ramasamy et al. reformed a WLO using SCW at 450 °C and 221 bar, and atmospheric-pressure steam from 715 to 880 °C [30]. They mainly studied how the use of different catalysts influenced the gasification, no other temperatures or pressures were explored within the supercritical and compressed steam regions. The present work shows new insights about the potential of this technology to turn WLOs into valuable gases such as H_2 and CH_4. It first explores how this residue is gasified under steam and supercritical conditions (50–500 bar) at different temperatures (500–750 °C) and reaction times (0.21–1.87 min). This initial approach is then used as basis to face the two main objectives and novel contributions of the work. Firstly, the calculation of the produced amounts of the objective gases H_2 and CH_4 (and others) and their concentrations in the gaseous streams produced, and the influence of the investigated variables on both parameters. Secondly, the compiled information is used for developing an energetic analysis of the process that supports the search for the optimal conditions of H_2 and CH_4 production from WLO steam and supercritical water gasification. As far as we know, this is the first time that an energetic analysis of this WLO valorization method is reported.

2. Materials and methods

2.1. Materials

Most of assays in this work used the synthetic automotive engine WLO Repsol 5W40 as feeding oil. The oil was used in a diesel car engine with a runtime of 15,000 km. Its density was 0.85 g cm^{-3} and its elemental composition was 84.32 wt% carbon, 13.28 wt% hydrogen, 0.33 wt% nitrogen and 0.19 wt% sulfur (determined by combustion at 1000 °C in a LECO CHNS-932 equipment). Inorganic components in the WLO were analyzed by inductively coupled plasma optical emission spectroscopy. The used ICP-OES equipment was a Ultima II Jobin Yvon. The samples were exposed to acid decomposition inside closed vessels, using a Milestone Ethos-Plus microwave oven to control the temperature. The operating parameters were: RF generator (1100 W), argon was used as plasma, auxiliary and nebulizer gas, plasma gas flow, auxiliary gas flow and nebulizer gas flow were 12.0, 0.2 and 1.0 dm^3 min^{-1}, respectively, nebulization pressure was 2.95 bar.

Other WLOs were also used in complementary assays: synthetic Elf 5W30 (30,000 km), synthetic AD 10W40 (20,000 km), semi-synthetic Petronas 15W40 (15,000 km) and the so-called “Mixture” sample, which was collected in a mechanic garage from a tank containing mixtures of several different WLOs. Further information about the characteristics of the WLOs can be found in the ESI Section S1.

Before the gasification experiments the WLOs were filtered through a stainless steel membrane filter 0.5 μm pore size to remove the solid particles that they may contain.

2.2. Experimental process

2.2.1. Gasification

The flow gasification assays were carried out in the installation shown in Fig. 1.

A water stream pumped by a Ultra High Pressure Analytical HPLC Dual PistonPump ChromTech pump went through a preheater before

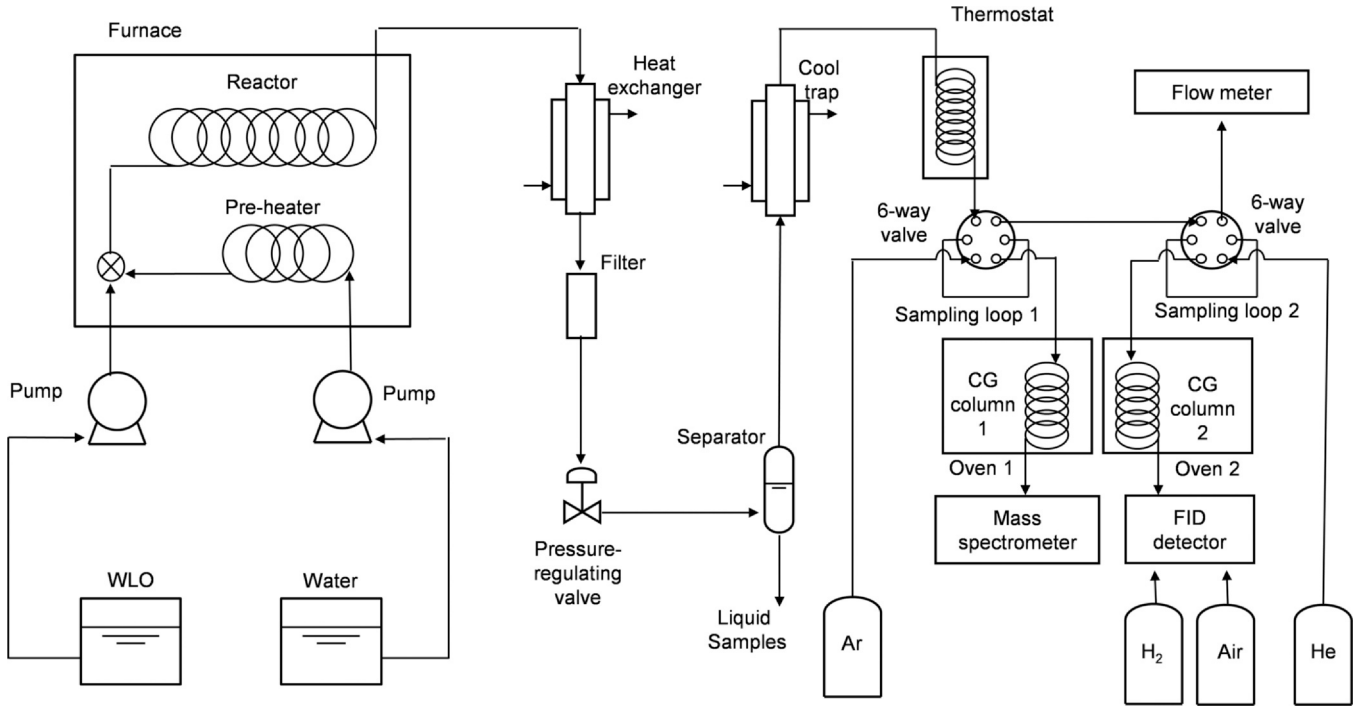

Fig. 1. Schematic of the installation used for the gasification experiments.

reaching a Hastelloy tubular reactor. The reactor consisted of a 16.8 cm^3 internal volume spring-manufactured tube (4.1 m length x 1/4" OD x 0.080″ wall). The reactor was situated inside of an electrical furnace and was heated to the reaction temperature. Once the reaction temperature had been attained, the used oil was pumped by a HPLC LabAlliance Series 1500 pump and was mixed with the water preheated to the reaction temperature at the entrance of the reactor. The stream leaving the reactor was cooled to ambient temperature by a cool water flow in a heat exchanger. It then went through a downstream filter and was discharged through a pressure-regulating valve. The installation allowed gasifying the WLO in a flow continuous process that, once stabilized, may be maintained during the desired time. In the present investigation, once the desired pressure and temperature were reached, the process was maintained for 60 min. At the end of each experiment the installation had to be cleaned in order to avoid obstructions due to the formation of char. The reaction time of each assay was calculated by approaching the density of the mixture to that of pure water at the same reaction pressure and temperature.

The reaction time (t) was calculated by the following equation, Eq. (1):

$$t = \frac{V_r \bullet \rho_{P,T}}{\dot{m}_{feeding}} \quad (1)$$

Where Vr is the internal volume of the reactor, $\rho_{T,P}$ is the water density at reaction conditions and $m_{feeding}$ is the mass flow feeding the reactor ($g_{water+oil}$ min^{-1}).

The pressure and temperature ranges analyzed spread from 50 bar to 500 bar, and from 500 °C to 750 °C, respectively. Assays at pressures below 50 bar could not be carried out because the corresponding reaction times were not long enough to be suitably compared to the reaction times achieved at higher pressures.

wt% was calculated as follows, Eq. (2):

$$wt(\%) = \left(\frac{oil\ mass\ flow\ feeding}{oil\ mass\ flow\ feeding\ +\ water\ mass\ flow\ feeding} \right) x\ 100 \quad (2)$$

The wt% range investigated was from 0.85% to 1%. These wt% values correspond to oil:water ratios from 1:100 to 1:83. Lower ratios could not be experimented because the amounts of gas generated by greater oil flows could not be managed in the available installation.

2.2.2. Analysis of the produced gaseous stream

The gas flow generated, the composition of the gas mixture and the concentration of each individual gas were determined in each assay. The gas flow went through a few conditioning stages before being analyzed. The effluent liquid and gas streams were first separated in a gas-liquid separator. The gas stream was then cooled to − 20 °C to retain the remaining humidity and it was finally heated at 30 °C. The concentrations of gases (vol%) were calculated combining the data obtained in (i) a Shimadzu GC-2010 Plus gas chromatograph with a H_2 flame ionization detector, and (ii) a GC-MS system consisting of a Teknokroma TR-GC1102010 chromatographic column and an Omnistar GSD 300 mass spectrometer. Further explanation about the analytical experimental procedure is detailed in [32]. The analyzed gases were H_2, CO, CO_2, CH_4, ethane, ethylene, acetylene (the sum of ethane, ethylene, and acetylene is shown as C_2), propane, propylene (the sum of propane and propylene is shown as C_3) and butane. The generated flow of gases was continuously measured in a Resteck Pro-Flow 6000 electronic flowmeter.

The gasification efficiency was evaluated from carbon gasification efficiency (CGE), Eq. (3), which could be calculated by characterizing the gaseous effluent:

$$CGE = \left(\frac{carbon\ mol\ flow\ in\ the\ produced\ \ gas}{carbon\ mol\ flow\ in\ the\ oil\ feeding} \right) \quad (3)$$

Gas Yield was defined as follows, Eq. (4):

$$Gas\ Yield\ = \left(\frac{\dot{m}_{produced\ gas}}{\dot{m}_{feeding\ oil}} \right) \quad (4)$$

Where $\dot{m}_{produced\ gas}$ (g_{gas} min^{-1}) is the mass flow of the produced gas and $\dot{m}_{feeding\ oil}$ (g_{oil} min^{-1}) the mass flow of oil feeding the reactor.

CGE and Gas Yield are not strictly comparable because of their different units but the comparison of their trends allows reaching conclusions about the extent of cracking and reforming reactions implied in gasification.

Regarding the energy aspects of gasification, Energy Recovery (ER), kJ kJ^{-1}, was defined as follows, Eq. (5):

$$Energy\ Recovery\ (ER) = \frac{Energy\ flow_{gas}}{Energy\ flow_{feeding\ oil}} \quad (5)$$

Where Energy $flow_{gas}$ (kJ min^{-1}) and Energy $flow_{feeding\ oil}$ (kJ min^{-1}) are the energy flows of the gas stream produced and the feeding oil, respectively. Energy flow is calculated as the product of the Higher Heating Value (HHV, kJ kg^{-1}) and the mass flow (kg min^{-1}) of the corresponding stream.

Energy Efficiency, EE, kJ kJ^{-1} was defined as follows, Eq. (6):

$$Energy\ Efficiency\ (EE) = \left(\frac{Energy\ flow_{gas}}{Energy\ Input}\right) \quad (6)$$

Where Energy Input is an estimation of the amount of energy spent in the process (kJ min^{-1}), Eq. (7):

$$EnergyInput_{P,T} = watermassflowfeeding \times [h_{T,P} - h_{20°C,1bar}]_{water} + WLOmassflowfeeding \times [h_{T,P} - h_{20°C,1bar}]_{WLO}] \quad (7)$$

ER and EE can be also calculated using the Lower Heating Value of the produced gases. Further information about the calculation of ER and EE and the differences arising from using HHV or LHV are described in ESI Section S2.

Error bars shown in the graphics refer (i) standard error (SD) for each specific gasification conditions to characterize the gases and (ii) the relative standard error of the analytical techniques used to characterize the liquid samples. Further information about their calculation is contained in the ESI Section S3.

2.2.3. Analysis of the produced liquid stream

The produced liquid stream and WLOs were characterized by gas chromatography with mass spectrometry (GC–MS) on an Agilent 7890a chromatograph equipped with an MS detector with an ionic trap Agilent MS220. 1 μL sample was extracted with 1 mL of ethyl acetate and then, 1 μL of the extract was injected in the chromatograph with a split ratio 20:1. An Agilent VF-5 chromatographic column was used, with a length of 30 m; an internal diameter of 0.25 mm; and a thick layer of 25 μm, with 25 mL min^{-1} of He as the carrier gas. The injector was maintained at 270 °C, and the following temperature program was used in the oven: an initial temperature of 50 °C maintained for 5 min, followed by heating at 10 °C min^{-1} to 270 °C, which was finally maintained for 5 min. The detection mode was selected as electronic impact ionization. Masses from 50 to 500 uma were recorded.

3. Results and discussion

3.1. Carbon gasification efficiency

CGE is a parameter associated with the conversion of the carbon contained in the oil to carbon-containing gases, so that it allows evaluating the efficiency of the gasification. Gas Yield allows evaluating the total production of gases, including the non carbon-containing too.

The effect of temperature on CGE and Gas Yield for treatments at supercritical conditions 250 bar, 0.3 min and 0.85 wt% is shown in Fig. 2a. The increase in temperature caused an increase in the conversion of carbon from the raw material to gaseous products. This increase was essentially linear from 500 °C to 600–650 °C, a temperature above which the increases in CGE were progressively smaller. Above 650 °C, Gas Yield behaved in a different way that CGE, since it kept increasing in a linear trend within the whole range assayed.

The mechanisms through which SCW gasifies linear hydrocarbons, which constitute the main fraction of the WLO, were thoroughly analyzed in previous studies [31]. The two main reactions involved in the conversion of hydrocarbons to gases are thermal cracking, Eq. (8), and hydrothermal reforming, Eq. (9).

$$C_xH_y \rightarrow \alpha\ C_aH_{2a+2} + \beta\ C_bH_{2b} + \gamma\ C_cH_{2c} + others \quad (8)$$

$$C_xH_y + x\ H_2O \rightarrow x\ CO + (x + 0.5\,y)\ H_2 \quad (9)$$

Both them have an endothermic nature, as revealed when a possible cracking route and the hydrothermal route are defined for a specific linear hydrocarbon like decane, Eqs. (10) and (11).

$$C_{10}H_{22} \rightarrow 2\ CH_4 + 3C_2H_4 + C_2H_2\ \Delta H^0_{25\ °C} = +\ 486.2\ kJ\ mol^{-1} \quad (10)$$

$$C_{10}H_{22} + 10H_2O \rightarrow 10\ CO + 21H_2\ \Delta H^0_{25\ °C} = +\ 1562.5\ kJ\ mol^{-1} \quad (11)$$

The endothermic nature of these two main reactions, CGE and Gas Yield increased with temperature. In a subsequent step, CO can be reformed by water (in excess) to produce CO_2 and further H_2 through the water-gas shift reaction. This reaction is exothermic under standard conditions, Eq. (12).

$$CO + H_2O \leftrightarrow CO_2 + H_2\ \Delta H^0_{25\ °C} = -\ 41.1\ kJ\ mol^{-1} \quad (12)$$

However, when the reforming takes place under supercritical conditions its thermodynamic nature changes from exothermic to endothermic: radical mechanisms prevail over ionic mechanisms due to the low ionic product of water under these conditions. Consequently, reaction kinetics of water-gas shift reaction are faster than under steam conditions without requiring catalyst, and they increase with temperature [27]. That dependence of water-gas shift reaction on temperature implied that, although the amounts of CO produced in the system at 650 and 750 °C were similar according to the behavior of CGE, the conversion of CO to CO_2 and H_2 was more efficient at 750 °C. As non-carbon containing H_2 production was greater at 750 °C, Gas Yield was greater than at 650 °C although CGE did not change significantly between both temperatures.

According to that, CGE and Gas Yield were respectively 0.48 mol C_{gas} mol C_{oil}^{-1} and 0.49 g_{gas} g_{oil}^{-1} at 600 °C, whereas at the highest temperature investigated they differed, being 0.60 mol C_{gas} mol C_{oil}^{-1} and 0.94 g_{gas} g_{oil}^{-1} respectively. The study of the concentrations of the gaseous species (see Section 3.2) verified the increase of H_2 concentration with temperature.

Fig. 2b shows the effect of pressure on gasification at 700 °C and 0.85 wt% for 0.3 min. The pressure range investigated included three pressures in the steam region, 50, 100 and 150 bar, and two pressures in the supercritical region, 250 and 500 bar. CGE slightly increased in the steam region from 50 to 150 bar. The enhanced diffusion coefficient and particle collision rate promoted by the pressure increase led to gasify greater amounts of WLO. Both phenomena should be more evident when higher pressures were used, but above 150 bar the gasification progressively slowed down until the highest pressure investigated in the supercritical region, 500 bar. In order to search for an explanation to this trend, the liquid effluents of each experiment were collected and analyzed (see ESI Section S4). Polycyclic aromatic hydrocarbons (PAHs) and phenol were detected; the concentrations of naphthalene, phenanthrene and pyrene were the greatest among the PAHs, although some others polycyclic compounds such as indene, fluorene or anthracene were also detected in negligible concentrations. The PAHs and the phenol contained in the liquid increased with pressure (Fig. S7). Previous investigations reported the formation of PAHs as a hurdle for gasification [31–34], since once these compounds are formed they are difficultly gasified and promote the formation of char. That is to say, highly pressurized water enhanced gasification through the improvement of mass transfer phenomena, but simultaneously hindered it by strongly promoting the, cyclization and aromatization of aliphatic hydrocarbons of the WLO, Eq. (13). These opposite effects resulted in a maximum CGE at 150 bar. It must be emphasized that this counter-productive cyclization effect is noted for linear hydrocarbons, but should not influence the gasification of other species with non-linear nature.

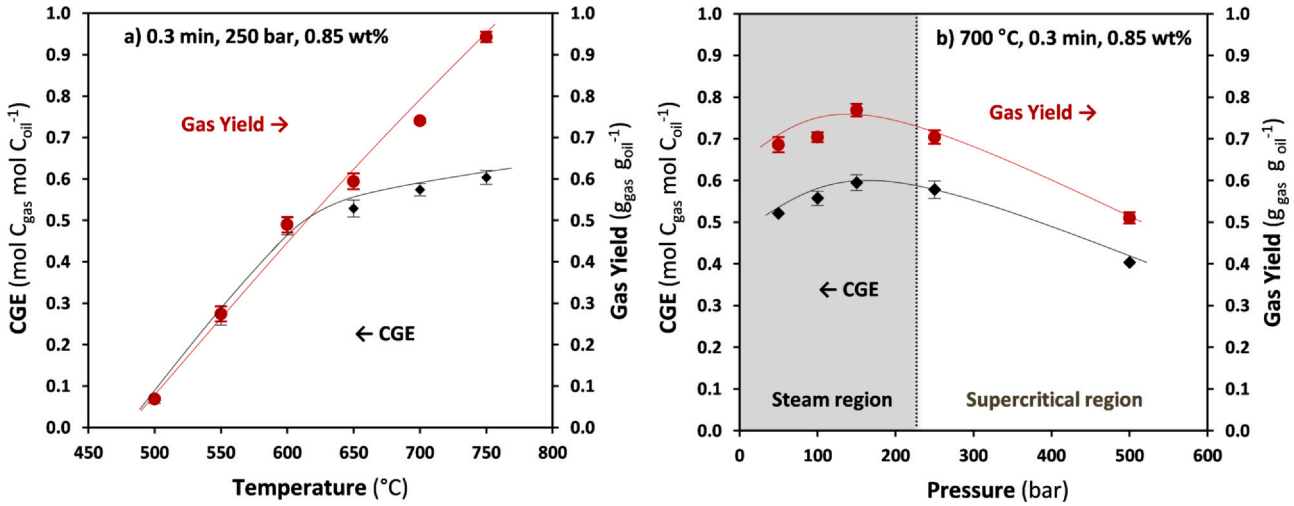

Fig. 2. (a) Effect of temperature on CGE and Gas Yield at 0.3 min, 250 bar and 0.85 wt%. (b) Effect of pressure on CGE and Gas Yield at 700 °C, 0.3 min and 0.85 wt%.

$$C_xH_{2x+2} + C_xH_{2x} + \text{others}_{\text{(light and intermediate HC)}} \rightarrow \text{naphthalene} + \text{phenantrene} + \text{others} \quad (13)$$

The trend of Gas Yield coincided with CGE, tracing a maximum at about 150 bar. Gas Yield was higher than CGE for all the pressures assayed, what reflected a remarkable reforming of the hydrocarbons contained in the WLO.

Fig. 3 reports the effect of time on CGE and Gas Yield for the supercritical gasification of WLO at 750 °C, 250 bar and 0.85 wt%. Remarkable changes in CGE for different reaction times were not observed under the conditions assayed, thus suggesting that for that high temperature the maximum gasification was achieved after approximately 12 s. Just a slight increase in Gas Yield was observed for the longest reactions, pointing that reforming pathways kept happening slowly as reaction time was lengthened. It must be noted that CGE as well as Gas Yield reached lower values than those reached by the corresponding fresh oil [32]. Those differences may arise as a result of some minor fractions contained in the WLO.

Firstly, PAHs concentration in the WLO was greater than in the fresh oil (see ESI Section S1). Furthermore, although the WLO was filtered with a 0.5 μm pore size filter before gasification, inorganic species like Ca and P, and heavy metals like Zn were identified in the feeding oil, Table 1.

Although the available installation did not allow quantifying the total amount of char produced in each assay, the solid residue accumulated on the filter after several assays was collected and analyzed to determine its elemental composition and inorganic content, following the same procedures used to characterize WLO. The H/C ratio of the char (79.75 wt% carbon, 3.44 wt% hydrogen, 0.32 wt% nitrogen and 0.80 wt% sulfur) was low, a typical characteristic of aromatic structures, what reinforced the idea of PHAs as promoters of char formation. The inorganic content was clearly higher than in the WLO: Ca/P and Zn concentrations were 9-folded and 7.5-folded increased respectively. The liquid effluents were also analyzed but the concentrations of these species were negligible. That implied that these inorganic species accumulated as a solid residue and also became a part of the char.

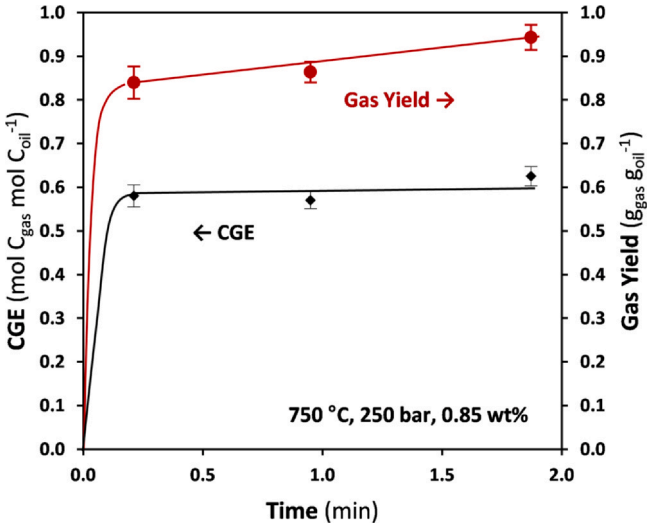

Fig. 3. Effect of reaction time on CGE and Gas Yield at 750 °C, 250 bar and 0.85 wt%.

Table 1
Elemental analysis ICP-OES of 5W40 WLO and the charred residue produced in its gasification.

Metal (ppm)	WLO	Charred residue
Al	8.3	*
Ca	1771	16,594
Fe	49.9	268
Mg	4.7	*
Cr	1.3	*
Ni	0.771	340
Pb	1.4	*
Zn	1022	7618
P	756.6	6315
S	1921	6393

The asterisk means that these metals have not been detected in the sample.

In summary, the presence of aromatic compounds and inorganic species and metals in the feeding may explain the lower CGEs achievable for the WLO, and these lower CGEs were rapidly achieved when high temperatures were employed.

In order to assess if the results with WLO 5W40 were applicable to other similar residues, supercritical gasification assays were carried out at 750 °C, 250 bar and 0.85 wt% for 0.3 min with other three different WLOs and one mixture. Table 2 shows the obtained results.

CGE and Gas Yield were highly reproducible for the five residues investigated. Both parameters were slightly higher for AD 10W40 and Petronas 15W40, but the differences were below 5–10%. As the results did not seem to be strongly influenced by the feeding oil, it can be stated that the gasification of other types of automotive WLO should behave similar to what is shown herein. However, it must be highlighted that the compositions of lube oils vary depending on their specific scope as automotive engine oils, industrial oils, aviation oils or metal working fluids [35]. Consequently, although our results seem to

Table 2
CGE and Gas Yield of the supercritical gasification of different WLOs at 750 °C, 250 bar, 0.3 min, 0.85 wt%.

WLOs	CGE (mol C_{gas} mol C_{oil}^{-1})	Gas Yield (g_{gas} g_{oil}^{-1})
Repsol 5W40	0.57 ± 0.01	0.91 ± 0.03
Elf 5W30	0.59 ± 0.02	0.90 ± 0.05
AD 10W40	0.63 ± 0.03	1.06 ± 0.04
Petronas 15W40	0.63 ± 0.02	1.07 ± 0.03
Mixture	0.60 ± 0.01	0.95 ± 0.02

be applicable to other automotive WLOs, the gasification of other types of WLOs may result different.

3.2. Production yields of H_2, CH_4 and other volatile hydrocarbons

The production yield of the different species produced in gasification depends on CGE, whose behavior is commented in the previous section, and the concentration of each species in the gaseous mixture. The influence of temperature over the concentration and the production yield of the gases obtained in the supercritical gasification of WLO Repsol 5W40 at 250 bar is shown in Fig. 4.

At temperatures below 600 °C, the gaseous mixture was mainly composed by volatile hydrocarbons such as CH_4, C_2, C_3 and butane (Fig. 4a), thus revealing that under such conditions the thermal cracking of the hydrocarbons contained in the WLO was the most important reaction in the system. The production of those gases was also valuable since they can be used as fuels, although the main scope of this investigation was the production of gases with a great HHV and a more environmentally sustainable nature like H_2 and CH_4.

As temperature increased the concentrations of butane, C_3 and C_2 decreased, what may be interpreted as an evidence of their conversion into other products, Fig. 4a. Simultaneously to the decrease in the concentrations of volatile hydrocarbons, other gases like H_2 and CO_2 began to be detected in the mixture. These gases were formed in the reforming reactions with water, which were favored at high temperatures because of their endothermic nature. In these reactions the involved reagents (besides water) were light hydrocarbons as well as intermediate compounds coming from cyclization and condensation reactions. Furthermore and as previously described, water-gas shift reaction reached higher conversions at high temperatures. As a result of the concomitant effect of all these pathways, the gaseous mixture obtained as temperature increased contained small amounts of CO, whereas the concentrations of CO_2 and H_2 were progressively higher. CH_4 was an intermediate product that took part in several simultaneous reactions and because of that, the explanation to its concentration trend was not so clear. It increased with temperature up to 700 °C since it was being produced in the thermal cracking of heavy hydrocarbons; when gasification was carried out at 750 °C it decreased softly probably as CH_4 began to be reformed, although this concentration hardly varied within this temperature range. In summary, the results showed that high temperatures, above 700 °C, where necessary to achieve a gaseous mixture in which H_2 and CH_4 predominated.

Fig. 4b shows how the production yield, units mol_{gas} g_{oil}^{-1}, of the different gases varied with temperature. In this figure the yields of the species C_2, C_3 and butane were gathered as C_2-C_4 to make the interpretation of the results easier. The production of H_2 increased with temperature because of the increase in its concentration (Fig. 4a) and in Gas Yield (Fig. 2a). This trend was especially remarkable from 650 to 750 °C, since at the highest temperature of this range the H_2 production yield was 7.5 times greater than at the lowest. The CH_4 production yield also increased within the whole temperature range assayed, in spite of the decrease in its concentration from 700 to 750 °C. CGE did increase within this range, so that the net yield increased thanks to the greater gasification of the WLO. The concentration and CGE also affected the production of volatile hydrocarbons C_2-C_4 in opposite ways. That is to say, an increase in the production of these gases was observed at the lowest temperatures, reaching a 1.15 10^{-2} mol_{gas} g_{oil}^{-1} maximum at 600 °C. The greater gasification of the WLO allowed the production yield to keep increasing until that temperature although their concentrations began to decrease above 550 °C. Above 600 °C and despite the increase in CGE, the volatile hydrocarbons production yield began to decrease, this turning point coinciding with a huge decrease in their concentrations. By this way, the greatest production of gases was associated to the highest temperature investigated, 750 °C. Namely, in the gasification of a WLO:water mixture 0.85 wt% at 750 °C and 250 bar for 0.3 min, 60% of the WLO was gasified (0.60 mol C_{gas} mol C_{oil}^{-1}) and the following yields of valuable gases were achieved: 2.94 10^{-2} g_{H2} g_{oil}^{-1}, 3.48 10^{-1} g_{CH4} g_{oil}^{-1}, 2.30 10^{-2} g_{CO} g_{oil}^{-1} and 1.53 10^{-1} $g_{C2\text{-}C4}$ g_{oil}^{-1}.

Taking into account the results of Fig. 4, the investigations in which the influence of pressure and time were analyzed were carried out only at high temperatures in order to search for maximum H_2 and CH_4 productions. Fig. 5a shows the influence of pressure on the concentration of the gases obtained in the gasification of the WLO at 700 °C, 0.3 min and 0.85 wt%.

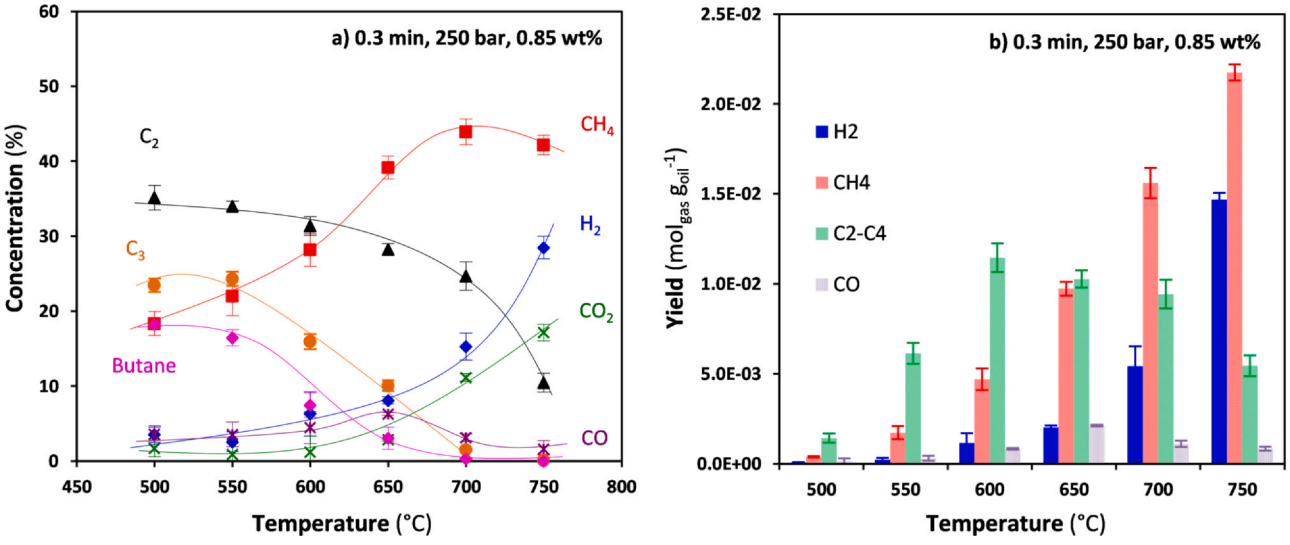

Fig. 4. Effect of temperature at 0.3 min, 250 bar and 0.85 wt% on (a) the concentrations of the species produced for gasification, (b) the production yields of H_2, CH_4 and other volatile hydrocarbons.

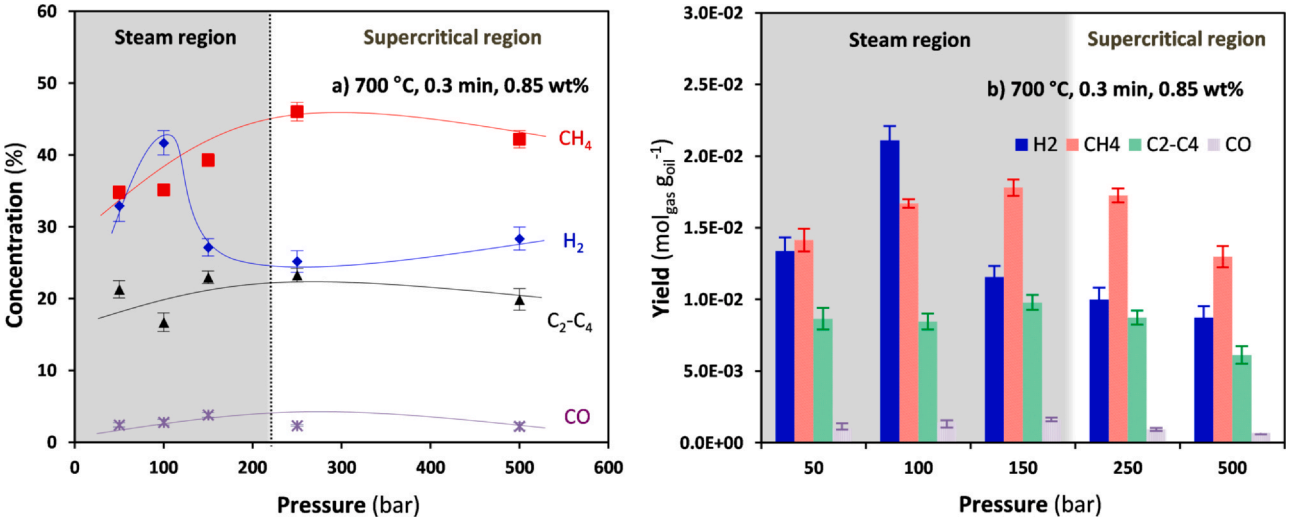

Fig. 5. Effect of pressure at 700 °C, 0.3 min and 0.85 wt% on (a) the concentrations of the species produced for gasification, (b) the production yields of H_2, CH_4 and other volatile hydrocarbons.

The concentrations of CO, C_2, C_3 and butane were low. The sum of C_2-C_4 did not change significantly as pressure increased from compressed steam at 50 bar to pressures inside the supercritical region until 500 bar. The yields of these gases showed similar trends from steam gasification at 50 bar until supercritical gasification at 250 bar, Fig. 5b. For higher pressures a slight decrease was observed related to the remarkable deceleration of CGE observed for the highest pressures assayed. The concentration of H_2 increased in the steam region from 50 to 100 bar, pressure at which its highest concentration was achieved, 41.7%. This high H_2 concentration together with the high CGE observed at this pressure in Fig. 2b suggested that the reforming of the hydrocarbons (Eq. (9)) was especially remarkable under these conditions. Above this pressure its concentration began to decrease until 250 bar, and then remained almost unchanged in the supercritical region. A similar trend was observed for H_2 production yield in Fig. 5b. Although Gas Yield slightly increased from 50 to 150 bar (Fig. 2b), the remarkable decrease in the concentration of H_2 within this range made this species yield decrease. The concentration of CH_4 traces an increase when the mixture was compressed to 250 bar and above that pressure described a plateau. CH_4 production yield increased from 50 to 150 bar although its concentration even increased until 250 bar; at higher pressures, it remained almost unchanged and slightly decreased for the highest pressure, 500 bar. This was again caused because the decrease in CGE, Fig. 2b.

In this study at 700 °C, the highest H_2 production, 4.22 10^{-2} g_{H2} g_{oil}^{-1}, was achieved in the compressed steam region at 100 bar. Other valuable gases were additionally produced such as CH_4, 2.67 10^{-1} g_{CH4} g_{oil}^{-1}, volatile hydrocarbons, 2.43 10^{-1} $g_{C2\text{-}C4}$ g_{oil}^{-1} and CO, 3.97 10^{-2} g_{CO} g_{oil}^{-1}. That is to say, 0.590 g of valuables gases per each gram of treated WLO were produced, and 55% of the WLO was gasified, 0.557 mol C_{gas} mol C_{oil}^{-1}. As the mixture was compressed until supercritical conditions, 250 bar, and once inside the supercritical region, 500 bar, a noticeable decrease in the production of valuable gases was recorded. Namely, at 500 bar 0.420 g of H_2, CO, CH_4 and C_2-C_4 were produced per each gram of treated WLO; that is to say, a 28.8% smaller production than at 100 bar.

Fig. 6a shows the effect of reaction time on the concentration of the gases for supercritical gasification at 750 °C, 250 bar and 0.85 wt%.

The concentration of H_2 increased as the reaction time was lengthened until reaching a 38.1% value for the longest time assayed, 1.87 min. CH_4 increased from 44.1% to 53.1% when the reaction was lengthened from 0.21 to 0.95 min. Its concentration traced a maximum

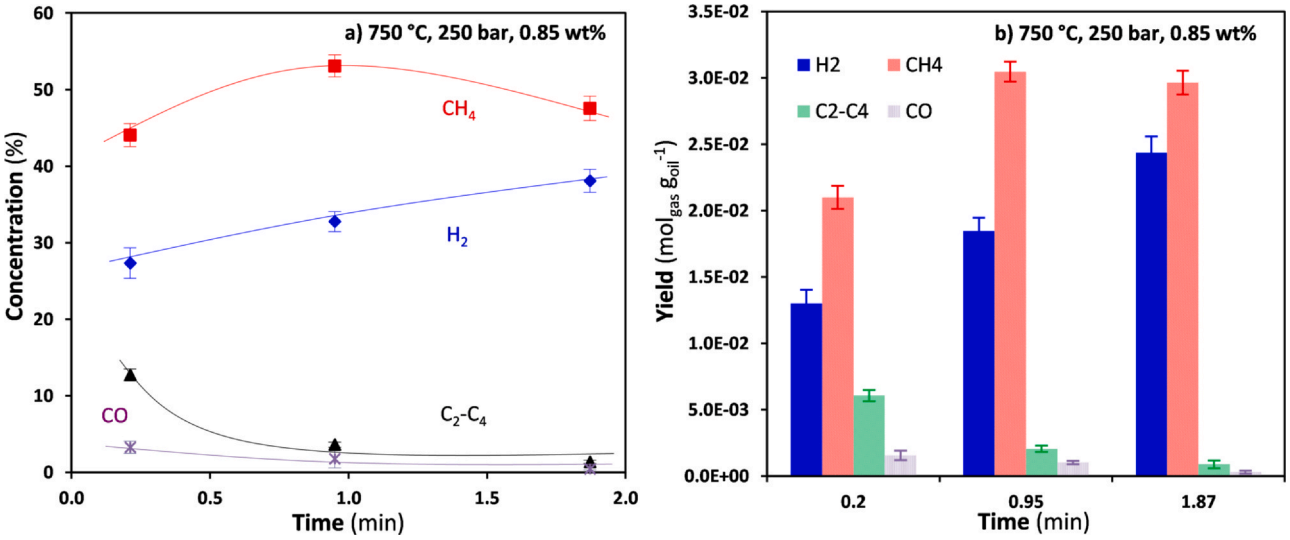

Fig. 6. Effect of reaction time at 750 °C, 250 bar and 0.85 wt% on (a) the concentrations of the species produced for gasification, (b) the production yields of H_2, CH_4 and other volatile hydrocarbons.

at this reaction time and then decreased softly. C_2-C_4 underwent a clear decrease until 0.95 min and the later trend was a plateau with concentrations below 4%. As previously commented, under these conditions the gasification of WLO was extremely fast since at reaction times longer than 0.2 min changes in CGE were not observed (Fig. 3). This meant that for longer reaction times, the reforming of the hydrocarbons formed in the thermal cracking were the only reaction pathways occurring. As a result of the reforming, it was observed that for the longest reaction time the concentration of the hydrocarbons and H_2 were, respectively the lowest and the highest. These results were especially interesting regarding the separation and purification of the gaseous mixture produced. High conversion degrees of the reforming reactions reduce the number of species contained in the mixture, thus facilitating their separation. This mixture composition can be compared with the complex mixtures obtained under other conditions such as, for example, 600 °C (Fig. 4a), a temperature at which six species had concentrations above 5%.

The data referring the production yields of valuable gases is shown in Fig. 6b. Since CGE hardly changed throughout the range of reaction times assayed, these results exclusively depended on the concentration of the gases. The enrichment of the mixture in H_2 became into greater amounts of H_2 produced per each gram of treated WLO; CH_4 yield increased at the earliest moments of the gasification and then decreased slightly; and the amounts of C_2-C_4 obtained for 0.95 and 1.87 min treatments were negligible. It was proved that an increase in the reaction time from 0.21 min to 1.87 min allowed achieving 46% more H_2 ($4.87\ 10^{-2}$ g_{H2} g_{oil}^{-1}) and 29% more CH_4 ($4.74\ 10^{-1}$ g_{CH4} g_{oil}^{-1}) using the same amount of WLO. $2.48\ 10^{-2}$ $g_{C2\text{-}C4}$ g_{oil}^{-1} and $8.21\ 10^{-3}$ g_{CO} g_{oil}^{-1} were also obtained, so that 0.556 g of valuable gases were obtained per each gram of treated WLO in a process with a high selectivity to H_2 and CH_4.

It is important to highlight that, although complete gasification of the WLO was not achieved, the concentration of PAHs and phenol in the liquid residue experienced a decrease as longer reaction times were assayed (see ESI Fig. S8). That is to say, the amounts of pollutant by-products leaving the reactor were smaller. The analytical results were supported by the appearance of the samples, Fig. 7. The feeding WLO's black color has been associated to the presence of aromatic compounds [36,37]. The color of the liquid effluent clearly changed as reaction time was lengthened, turning from a brown liquid after 0.21 min of treatment to yellowish tonalities after 1.87 min.

The concentration of the produced gases, Table 3, and the H_2 and CH_4 production yields, Table 4, were also investigated for other WLOs under the following supercritical gasification conditions: 750 °C; 250 bar, 0.3 min and 0.85 wt%. As the data collected in both tables show, small differences in these parameters were observed for the different WLOs investigated. The gasification of Petronas 15W40 and AD 10W40 resulted in H_2 production yields slightly higher than in the other three WLOs, although it can be stated that the specific type of automotive WLO does not change the concentrations nor the production yields significantly.

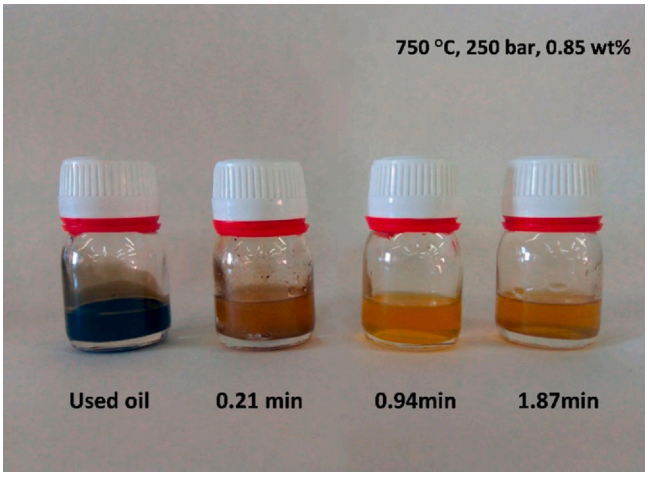

Fig. 7. Comparison of the color of liquid samples from WLO at different reaction time gasification. (For interpretation of the references to color in this figure legend, the reader is referred to the web version of this article.)

Besides this experimentation, an alternative series of assays at 750 °C was carried out to evaluate the efficiency of the production of H_2 and CH_4 from another perspective. In this case, the same flows of water and WLO were used in all cases, 1 cm^3 min^{-1} of water and 0.012 cm^3 min^{-1} of WLO, but the pressure was varied from 50 to 500 bar. Table 5 collects the reaction times achieved at each pressure (directly depending from the changes in the density of water) and the production of gases.

Thanks to the higher densities associated to the supercritical fluid, longer reaction times were achieved in the treatments at high pressures. By this way, a 2 min reaction could be achieved when gasifying at supercritical pressure of 500 bar whereas for the same flows of water and WLO at, for example, steam pressure of 50 bar, the reaction time was 0.18 min Fig. 2b proves that gasification kinetics at steam conditions, 50–150 bar, were faster that under supercritical conditions, 250–500 bar. On the other hand, Fig. 3 shows that the highest Gas Yields were recorded at the longest reaction times. Furthermore, the unique properties of supercritical fluids contribute to highest conversion degrees in the reforming reactions of hydrocarbons, since the clusters of water molecules in supercritical state produce free H and OH radical that improve the production of H_2 [38]. Taking into account these opposite effects of pressure on the reaction time, the gasification kinetics and the production of gases, Table 5 shows that the longer reaction times achieved under supercritical conditions compensated their slower kinetics. Namely, the gasification at 500 bar and 2 min reaction time produced $2.49\ 10^{-2}$ mol_{H2} g_{oil}^{-1}, the highest value recorded for H_2 in this study, and $2.99\ 10^{-2}$ mol_{CH4} g_{oil}^{-1}, one among the highest CH_4 production yields. It is interesting to note that in the 500 bar experiment, the effluent gas stream contained a mass of atomic hydrogen equal to 0.169 g_H g_{oil}^{-1}, distributed between H_2 and CH_4, and this hydrogen content was 27% greater than the content of the feeding oil, 0.133 g_H g_{oil}^{-1}. This excess of hydrogen could only come from water, which seemed to play a key role in the improvement of the production of H_2. In fact, volatile hydrocarbons and phenol in the gas effluent, and PAHs and phenol in the liquid effluent were not included in this calculation, so the hydrogen enrichment caused by water may be even greater.

The technical drawbacks of supercritical technologies, such as the necessity for reactors with large-thickness made of expensive materials, among others, are well known. On the other hand, the described enrichment phenomenon was especially evident in SCW gasification thanks to the long reaction times achieved, and the faster kinetics of reforming reactions like water-gas shift reaction under these conditions. These conclusions meant that the long reaction times associated to SCW gasification allowed reducing the internal volume of the reactors in comparison to those required in steam gasification; or from another perspective, they allowed reaching higher process yields for the same internal volume of reactor.

3.3. Energy yields

Fig. 8 shows the changes in the energy indicators, ER and EE, as temperature was varied in supercritical gasification assays at 250 bar and 0.85 wt% for 0.3 min. A great influence of the temperature in both energetic indicators was observed; in general terms, both of them increased with temperature. For temperatures from 500 to 600 °C, the increases were more marked than at higher temperatures although they kept increasing until 700 °C. In the range from 700 to 750 °C EE hardly varied; ER was higher at 750 °C but the increase from 700 °C was not as noticeable as at low temperatures.

Table 3
Concentrations of species produced in the supercritical gasification of differents WLOs at 750 °C, 250 bar, 0.3 min and 0.85 wt%.

WLOs	H_2 (%)	CH_4 (%)	CO (%)	CO_2 (%)	C_2 (%)
Repsol 5W40	27.8 ± 1.8	40.8 ± 2.9	4.6 ± 0.4	18.6 ± 2.4	8.1 ± 0.9
Elf 5W30	27.3 ± 2.2	44.0 ± 3.0	5.8 ± 0.5	13.3 ± 2.3	8.9 ± 1.1
AD 10W40	28.5 ± 1.6	39.3 ± 3.0	6.3 ± 0.4	17.9 ± 3.6	6.8 ± 0.3
Petronas 15W40	29.2 ± 2.4	41.0 ± 2.0	5.2 ± 0.3	18.2 ± 3.4	5.7 ± 0.8
Mixture	26.1 ± 2.5	41.1 ± 3.6	4.3 ± 0.3	18.3 ± 3.2	9.8 ± 0.8

Table 4
H_2 and CH_4 production yields for the supercritical gasification of differents WLOs at 750 °C, 250 bar, 0.3 min and 0.85 wt%.

WLOs	H_2 yield 10^2 (mol_{H2} g_{oil}^{-1})	CH_4 yield 10^2 (mol_{CH4} g_{oil}^{-1})
Repsol 5W40	1.46 ± 0.01	2.08 ± 0.08
Elf 5W30	1.39 ± 0.03	2.29 ± 0.09
AD 10W40	1.64 ± 0.01	2.26 ± 0.08
Petronas 15W40	1.69 ± 0.02	2.38 ± 0.10
Mixture	1.32 ± 0.04	2.07 ± 0.07

It is evident that gasifying the WLO at high temperatures required the consumption of greater amounts of energy than at low temperatures; furthermore, the use of more resistant materials for manufacturing the reactors and a more rigorous maintenance of the installations became mandatory. However, the data show that the tough requirements of high temperatures were compensated by higher energetic efficiencies. For the conditions showed in Fig. 8, ER and EE doubled when heating from 550 to 700 °C. At 750 °C the values of ER and EE were 0.68 kJ kJ^{-1} and 0.072 kJ kJ^{-1}, respectively (0.61 kJ kJ^{-1} and 0.064 kJ kJ^{-1} if LHV is used in their calculations instead of HHV, see ESI Section S2). The high temperature processes were more efficient because under those conditions the reforming reactions that conducted to gases with large HHV such as H_2 and CH_4 were favored. The production of CH_4 and, above all, H_2 was boosted by the hydrogen contained in water. Consequently, the appliance of water as reaction medium and reactant revealed as critical in the search for the economical and energetic viability of this valorization method.

It must be remarked that the low EE values achieved are caused by the low wt% used in this investigation, which were limited by the available installation. This was not considered a major drawback since our goal was to analyze the effect of temperature, pressure and reaction time on those parameters rather than obtaining high EE values. However, it can be stated that the use of greater WLO flow would probably lead to higher EEs.

The effect of reaction time on the energy performance of the gasification under supercritical conditions was also analyzed, Fig. 9. After scarcely 0.2 min of gasification at 750 °C and 250 bar, 70% of the energy contained in the WLO was recovered as gas (60% if LHV is used in the calculation of ER instead of HHV, see ESI Section S2). Once this value was reached, ER remained unchanged as longer reaction times were explored. Nevertheless, the graphic shows a strong influence of reaction time on EE, since it seemed to increase tracing an almost linear trend throughout the whole range investigated. Consequently, although neither CGE nor ER increased after a certain reaction time, long

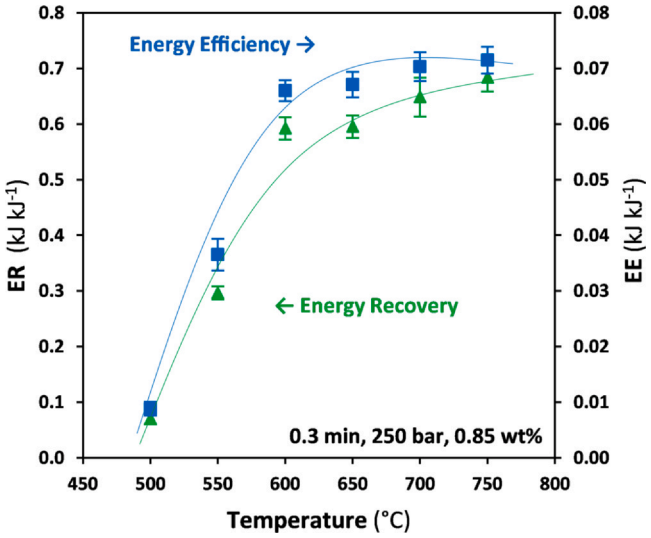

Fig. 8. Effect of temperature on EE and ER at 0.3 min, 250 bar and 0.85 wt%.

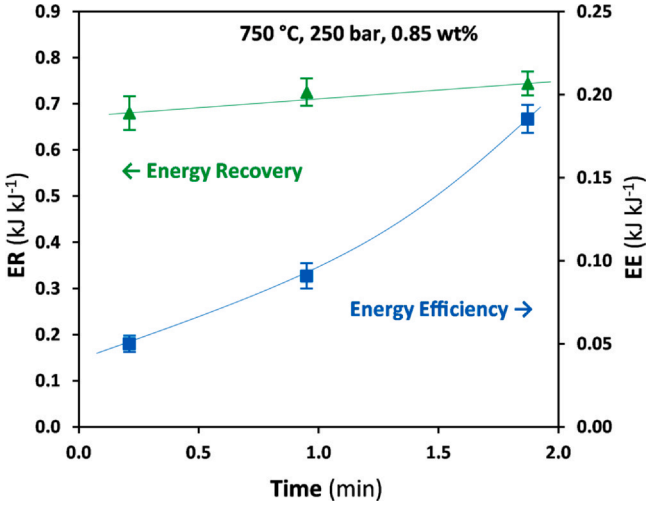

Fig. 9. Effect of reaction time on EE and ER at 750 °C, 250 bar and 0.85 wt%.

reactions led to the most favorable EEs. The increase in Gas Yield with time (Fig. 3) is here revealed as the cause of the trend of EE, which increases from 0.05 kJ kJ^{-1} after 0.2 min of reaction, to 0.19 kJ kJ^{-1} after 1.87 min, four times greater. Although reforming reactions were

Table 5
H_2 and CH_4 production yields for the steam and supercritical gasification of 0.012 cm^3 min^{-1} of WLO and 1 cm^3 min^{-1} of water at 750 °C and different pressures (1 wt%).

Pressure (bar)	Water state	Time (min)	H_2 yield 10^2 (mol_{H2} g_{oil}^{-1})	CH_4 yield 10^2 (mol_{CH4} g_{oil}^{-1})
50	Steam	0.18	1.89 ± 0.04	1.95 ± 0.03
150	Steam	0.55	1.95 ± 0.07	2.93 ± 0.10
250	Supercritical	0.94	1.93 ± 0.08	2.96 ± 0.09
500	Supercritical	2.00	2.49 ± 0.07	2.99 ± 0.06

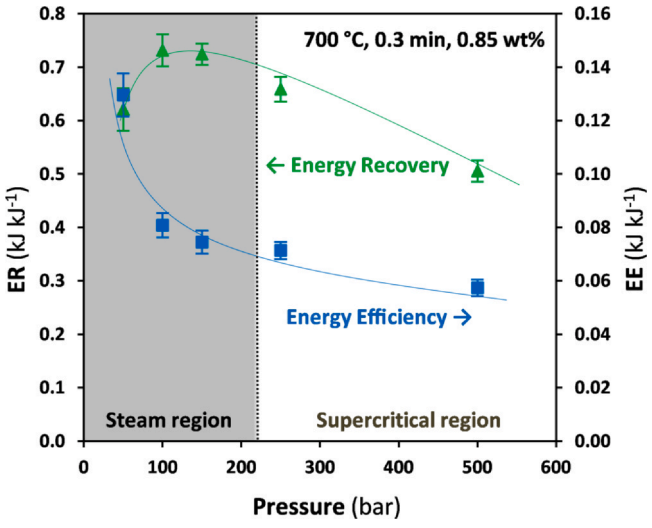

Fig. 10. Effect of pressure on EE and ER at 700 °C, 0.3 min and 0.85 wt%.

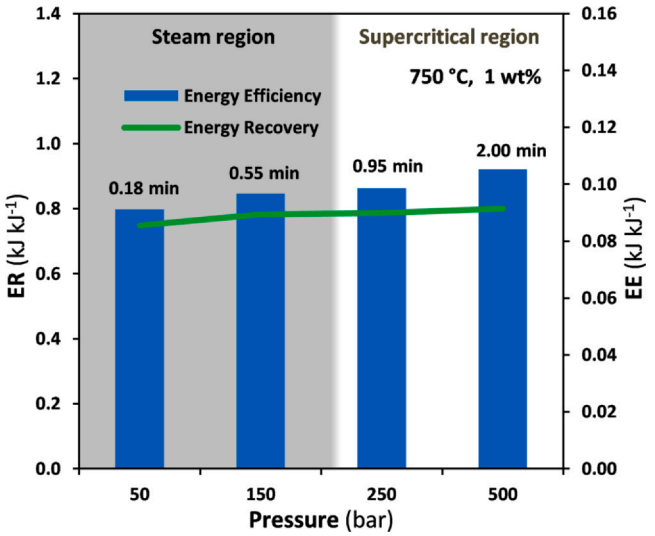

Fig. 11. Effect of pressure on EE and ER for the gasification of 0.012 cm^3 min^{-1} of WLO and 1 cm^3 min^{-1} of water at 750 °C (1 wt%).

slow, long enough reaction times were appropriate so that the volatile hydrocarbons could be reformed and turned into gases with large HHV as H_2. This strategy seemed to be the most suitable to develop an energetically efficient process.

Fig. 10 shows the changes in the energy parameters of gasification with pressure. ER showed a rising trend when the steam was compressed from 50 to 100 bar but then decreased progressively from steam gasification at 150 bar to supercritical gasification at 500 bar. EE decreased throughout the whole range studied, this decrease being sharper at the lowest pressures and softer but continuous inside the supercritical region. This trend was caused by several factors. Gasification kinetics slowed down with pressure (Fig. 2b) what could negatively affect EE due to a smaller gas flow. In addition, high water flows had to be used in the supercritical region than in the steam region to achieve the same reaction time because of the higher density of the fluid under those conditions; that is to say, the energy consumption associated to the heating of water was larger. As a result of a deficient production of gases with high HHV and large energy requirements, a noticeable diminution of EE with pressure was observed.

The previous comments refer a study in which the different assays employed different water and WLO flows to achieve the same reaction time at different pressures in the steam and supercritical regions. The relevance of the pressure on the energetic parameters could be also analyzed for assays employing the same water and WLO flows at different pressures and, consequently, different reaction times. Fig. 11 shows the effect of pressure on ER and EE for the gasification of 0.012 cm^3 min^{-1} of WLO using 1 cm^3 min^{-1} of water at 750 °C and different pressures.

The results obtained in this study were rather different since ER was essentially the same for all the pressures explored and EE slightly increased, in comparison with the clear decrease with pressure shown in Fig. 10. As previously commented, the longer reaction times achieved in the supercritical state compensated for its slower kinetics. The different amount of energy required to heat highly pressurized water also contributed to the improvement of the process regarding the use of steam (water enthalpy at 750 °C and 500 bar is 3777.2 kJ kg^{-1} whereas at 750 °C and 50 bar is 4021.7 kJ kg^{-1}), although this phenomenon was less important.

In summary, the results showed that the opposite of pressure on the gasification kinetics (high pressures, slow kinetics) and the reaction times reached (high pressures, long reaction times), finally made pressure to not influence the energy indicators significantly when the same flows of water and WLO were employed.

4. Conclusions

This work explored the gasification of WLO with water under steam and supercritical states. The influence of important variables like temperature, pressure and reaction time on the gasification efficiency, the production yields of valuable gases and the energetic performance of the process were investigated. Gasification assays with a few samples of automotive engine WLOs were carried out to analyze the reproducibility of the obtained results.

2.4 10^{-2} mol_{H2} $g_{oil}{}^{-1}$ and 3.0 10^{-2} mol_{CH4} $g_{oil}{}^{-1}$ were produced in the gasification of a WLO at 750 °C, 250 bar and 0.85 wt% for 1.87 min. Under these conditions, 62.5% of the feeding oil was gasified, the Gas Yield was 0.94 g_{gas} $g_{oil}{}^{-1}$, and the best energetic performance was recorded: EE was 0.19 kJ kJ^{-1} and ER was 0.74 kJ kJ^{-1}. wt% values were adapted to the maximum capacity of the experimental installation to manage gas flows, although higher wt% than those explored herein were expected to significantly improve EE.

It was concluded that high gasification temperatures were required to significantly obtain the two gases mainly pursued in this investigation, H_2 and CH_4. The greatest productions were achieved at the highest temperature explored, 750 °C, although the analysis of EE revealed that the increase in temperature above 650–700 °C did not involve a great improvement from the energetic point of view. The reaction time did not exert a significant influence on CGE under the high temperature conditions assayed, although it was a critical variable for the energetic performance. Long reaction times were interesting to improve the process energy indicators, namely EE, as much as possible. Regarding the effect of pressure, the assays carried out at the lowest pressures showed the fastest kinetics. However, the reaction times reached by compressed steam in flow tubular reactor were short in comparison with SCW; low H_2 and CH_4 production yields, large formation of products other than H_2 and CH_4, and low EEs were the consequences. High pressures inside the supercritical region, 500 bar, allowed reaching long reaction times that partially compensated their low kinetics, although these severe conditions involved other drawbacks, above all from a technical point of view. Consequently, intermediate pressures between 150 and 250 bar, seemed to be the most suitable (high concentrations of the targeted species, gas yield productions and energetic efficiencies) to obtained H_2 and CH_4 from the gasification of a WLO.

Declaration of Competing Interest

The authors declare that they have no known competing financial interests or personal relationships that could have appeared to influence the work reported in this paper.

Acknowledgments

Financial support from the Spanish Ministerio de Economía y Competitividad (Project CTQ2015-64339-R) and Anticipos Fondos Feder is acknowledged.

Appendix A. Supporting information

Supplementary data associated with this article can be found in the online version at doi:10.1016/j.supflu.2021.105267.

References

[1] K. Ramadass, M. Megharaj, K. Venkateswarlu, R. Naidu, Ecological implications of motor oil pollution: Earthworm survival and soil health, Soil Biol. Biochem. 85 (2015) 72–81, https://doi.org/10.1016/j.soilbio.2015.02.026
[2] D.C. Vargas, M.B. Álvarez, A. Hidrobo, K.M. Van Geem, D. Almeida, Kinetic study of the thermal and catalytic cracking of waste motor oil to diesel-like fuels, Energy Fuels 30 (2016) 9712–9720.
[3] C.T. Pinheiro, R.F. Pais, M.J. Quina, L.M. Gando-Ferreira, Regeneration of waste lubricant oil with distinct properties by extraction-flocculation using green solvents, J. Clean. Prod. 200 (2018) 578–587, https://doi.org/10.1016/j.jclepro.2018.07.282
[4] N.M. Nasim, S.M. Pervez, B.R. Yarasu, V. Lotia, Recycling waste automotive engine oil as alternative fuel for diesel engine: a review, IOSR-JMCE (2014) 46–50.
[5] T.E. Oladimeji, J.A. Sonibare, J.A. Omoleye, M.E. Emetere, F.B. Elehinafe, A review on treatment methods of used lubricating oil, Int. J. Civ. Eng. Technol. 9 (2018) 506–514.
[6] A. Demirbas, M.A. Balubaid, M. Reda, W. Ahmad, Diesel fuel from waste lubricating oil by pyrolytic distillation, Petrol. Sci. Technol. 33 (2015) 129–138, https://doi.org/10.1080/10916466.2014.955921
[7] X. Li, J. Zhai, H. Li, X. Gao, An integration recycling process for cascade utilization of waste engine oil by distillation and microwave-assisted pyrolysis, Fuel Process. Technol. 199 (2020) 106245, , https://doi.org/10.1016/j.fuproc.2019.106245
[8] S. Kim, J. Kim, J. Jeon, Y. Park, C. Park, Non-isothermal pyrolysis of the mixtures of waste automobile lubricating oil and polystyrene in a stirred batch reactor, Renew. Energy 54 (2013) 241–247, https://doi.org/10.1016/j.renene.2012.08.001
[9] G.J. Song, Y.C. Seo, D. Pudasainee, I.T. Kim, Characteristics of gas and residues produced from electric arc pyrolysis of waste lubricating oil, Waste Manag. 30 (2010) 1230–1237, https://doi.org/10.1016/j.wasman.2009.10.004
[10] I. Ahmad, R. Khan, M. Ishaq, H. Khan, M. Ismail, K. Gul, W. Ahmad, Valorization of spent lubricant engine oil via catalytic pyrolysis: influence of barium-strontium ferrite on product distribution and composition, J. Anal. Appl. Pyrolysis 122 (2016) 131–141, https://doi.org/10.1016/j.jaap.2016.10.008
[11] C. Acar, I. Dincer, Comparative assessment of hydrogen production methods from renewable and non-renewable sources, Int. J. Hydrog. Energy 39 (2014) 1–12, https://doi.org/10.1016/j.ijhydene.2013.10.060
[12] H. Jin, C. Fan, W. Wei, D. Zhang, J. Sun, C. Cao, Evolution of pore structure and produced gases of Zhundong coal particle during gasification in supercritical water, J. Supercrit. Fluids 136 (2018) 102–109, https://doi.org/10.1016/j.supflu.2018.02.016
[13] Y. Zhang, L. Li, P. Xu, B. Liu, Y. Shuai, B. Li, Hydrogen production through biomass gasification in supercritical water: a review from exergy aspect, Int. J. Hydrog. Energy 44 (2019) 15727–15736, https://doi.org/10.1016/j.ijhydene.2019.01.151
[14] R. Zhang, W. Jiang, L. Cheng, B. Sun, D. Sun, J. Bi, Hydrogen production from lignite via supercritical water in flow-type reactor, Int. J. Hydrog. Energy 35 (2010) 11810–11815, https://doi.org/10.1016/j.ijhydene.2010.01.029
[15] Y. Zhang, Y. Cui, P. Chen, S. Liu, N. Zhou, K. Ding, et al., Chapter 14 - Gasification technologies and their energy potentials, in: M.J. Taherzadeh, K. Bolton, J. Wong, A. Pandey (Eds.), Sustainable Resource Recovery and Zero Waste Approaches, Elsevier, 2019, pp. 193–206.
[16] G.A. Martínez, L.E.E. Silva, P.J.C. Escobar, O.A. Almazán del Olmo, Hydrogen production from oil sludge gasification/biomass mixtures and potential use in hydrotreatment processes, Int. J. Hydrog. Energy 43 (2018) 7808–7822, https://doi.org/10.1016/j.ijhydene.2018.03.025
[17] B. Zhang, L.R. Wang, Chapter 10 - Bioconversion and chemical conversion of biogas for fuel production, in: M. Hosseini (Ed.), Advanced Bioprocessing for Alternative Fuels, Biobased Chemicals, and Bioproducts, Woodhead Publishing, 2019, pp. 187–205.
[18] R.F. Susanti, L.W. Dianningrum, T. Yum, Y. Kim, Y.W. Lee, J. Kim, High-yield hydrogen production by supercritical water gasification of various feedstocks: alcohols, glucose, glycerol and long-chain alkanes, Chem. Eng. Res. Des. 92 (2014) 1834–1844, https://doi.org/10.1016/j.cherd.2014.01.003
[19] B. Yu, I. Chien, Design and economic evaluation of coal to synthetic natural gas (SNG) process, Comput. Aided Chem. Eng. 37 (2015) 1109–1114, https://doi.org/10.1016/B978-0-444-63577-8.50030-9
[20] G. Li, Z. Liu, F. Liu, Y. Weng, S. Ma, Y. Zhang, Thermodynamic analysis and techno-economic assessment of synthetic natural gas production via ash agglomerating fluidized bed gasification using coal as fuel, Int. J. Hydrog. Energy 45 (2020) 27359–27368, https://doi.org/10.1016/j.ijhydene.2020.07.025
[21] I. Staffell, D. Scamman, A. Velazquez, P. Balcombe, P. Dodds, P. Ekins, N. Shah, K. Ward, The role of hydrogen and fuel cells in the global energy system, Energy Environ. Sci. 12 (2019) 463–491, https://doi.org/10.1039/C8EE01157E
[22] M. Momeni, M. Soltani, M. Hosseinpour, J. Nathwani, A comprehensive analysis of a power-to-gas energy storage unit utilizing captured carbon dioxide as a raw material in a large-scale power plant, Energy Convers. Manag. 227 (2021) 113613, , https://doi.org/10.1016/j.enconman.2020.113613
[23] M.M. Jaffar, M.A. Nahil, P.T. Williams, Synthetic natural gas production from the three stage (i) pyrolysis (ii) catalytic steam reforming (iii) catalytic hydrogenation of waste biomass, Fuel Process. Technol. 208 (2020) 106515, , https://doi.org/10.1016/j.fuproc.2020.106515
[24] D. Wang, S. Li, S. He, L. Gao, Coal to substitute natural gas based on combined coal-steam gasification and one-step methanation, Appl. Energy 240 (2019) 851–859, https://doi.org/10.1016/j.apenergy.2019.02.084
[25] D.P. Chynoweth, J.M. Owens, R. Legrand, Renewable methane from anaerobic digestion of biomass, Renew. Energy 22 (2001) 1–8, https://doi.org/10.1016/S0960-1481(00)00019-7
[26] N. Lupton, L.D. Connell, D. Heryanto, R. Sander, M. Camilleri, D.I. Down, Z. Pan, Enhancing biogenic methane generation in coalbed methane reservoirs – core flooding experiments on coals at in-situ conditions, Int. J. Coal Geol. 219 (2020) 103377, , https://doi.org/10.1016/j.coal.2019.103377
[27] F. Rice, R. Steeper, J. Aiken, Water density effects on homogeneous water-gas shift reaction kinetics, J. Phys. Chem. A 102 (1998) 2673–2678, https://doi.org/10.1021/jp972368x
[28] B. Veriansyah, J. Kim, J.D. Kim, Y.W. Lee, Hydrogen production by gasification of isooctane using supercritical water, Int. J. Green Energy 5 (2008) 322–333.
[29] R. Rana, S. Nanda, J.A. Kozinski, A.K. Dalai, Investigating the applicability of Athabasca bitumen as a feedstock for hydrogen production through catalytic supercritical water gasification, J. Environ. Chem. Eng. 6 (2018) 182–189, https://doi.org/10.1016/j.jece.2017.11.036
[30] K.K. Ramasamy, A. T-Raissi, Hydrogen production from used lubricating oils, Catal. Today 129 (2007) 365–371, https://doi.org/10.1016/j.cattod.2006.09.037
[31] A.M. Sanchez, N. Martin, M.J. Sanchez, C. Izquierdo, F. Salvador, Effect of pressure on the gasification of dodecane with steam and supercritical water and consequences for H2 production, J. Mater. Chem. A Mater. Energy Sustain. 6 (2018) 1671–1681, https://doi.org/10.1039/C7TA09659C
[32] A.M. Sanchez, N. Martin, M.J. Sanchez, C. Izquierdo, F. Salvador, Different options to upgrade engine oils by gasification with steam and supercritical water, J. Supercrit. Fluids 164 (2020) 104912, , https://doi.org/10.1016/j.supflu.2020.104912
[33] J. Bae, S. Lee, S. Kim, J. Oh, S. Choi, M. Bae, I. Kang, S.P. Katikaneni, Liquid fuel processing for hydrogen production: a review, Int. J. Hydrog. Energy 41 (2016) 19990–20022, https://doi.org/10.1016/j.ijhydene.2016.08.135
[34] M. Gong, Y. Wang, Y. Fan, W. Zhu, H. Zhang, Y. Su, Polycyclic aromatic hydrocarbon formation during the gasification of sewage sludge in sub- and supercritical water: effect of reaction parameters and reaction pathways, Waste Manag. 72 (2018) 287–295, https://doi.org/10.1016/j.wasman.2017.11.024
[35] S.P. Srivastava, Classification of lubricants, in: S.P. Srivastava (Ed.), Developments in Lubricant Technology, Wiley Online Library, 2014, pp. 7–21.
[36] Y.M. Alshammari, K. Hellgardt, Sub and supercritical water reforming of n-hexadecane in a tubular flow reactor, J. Supercrit. Fluids 107 (2016) 723–732, https://doi.org/10.1016/j.supflu.2015.07.037
[37] T. Moriya, H. Enomoto, Characteristics of polyethylene cracking in supercritical water compared to thermal cracking, Polym. Degrad. Stab. 65 (1999) 373–386, https://doi.org/10.1016/S0141-3910(99)00026-9
[38] H. Jin, Y. Wu, C. Zhu, L. Guo, J. Huang, Molecular dynamic investigation on hydrogen production by furfural gasification in supercritical water, Int. J. Hydrog. Energy 41 (2016) 16064–16069, https://doi.org/10.1016/j.ijhydene.2016.04.214